

# SPACE MEASUREMENTS OF VERTICAL PROFILES OF TROPOSPHERIC MINOR CONSTITUENTS

Tadao Aoki

Meteorological Research Institute

Tsukuba, Ibaraki 305, Japan

## ABSTRACT

A method for remote measurement of tropospheric constituents from satellite is described, where the visible and near infrared solar radiation in the sunglint region is measured with tunable etalons and very narrow band pass filter which contains only one absorption line of trace gases concerned. The mathematical procedure is described to retrieve the vertical profiles of constituents. To study the feasibility of this method a ground based instrument has been developed and some results of remote measurements of water vapor are presented.

## I. INTRODUCTION

For nearly two decades the remote sounding of the tropospheric gases from satellite have been made by measuring the emission from the atmosphere and ground or sea surface. Since 1978 the TIROS-N satellite series has operationally been obtaining the water vapor vertical profile by measuring the infrared emission from the atmosphere with a filter type radiometer. The error is more than 20 percent near the ground and worse in the higher altitude (Timchak, 1986). The remote measurement of *CO* has been made by MAPS (Measurement of Air Pollution from Satellites) on board the space shuttle, also by measuring the infrared emission through gas filter. The accuracy has been estimated to be an order of 20 percent (Reiche et al., 1982).

In the future satellite program some new type of instruments such as a Fourier transform spectrometer and a grating spectrometer are proposed for remote sounding the tropospheric trace gases. These are again based on the measurement of thermal emission from the atmosphere. TERSE (Tunable Etalon Remote Sounder for the Earth) is a new vertical sounder for the tropospheric trace gases proposed by Aoki et al. (1989, 1993), where the near infrared solar radiation in the sun glint region is observed with tunable etalons where the separation of two etalon plates are changed with piezo electric elements. In this paper our recent work is summarized.

## II. RETRIEVAL ALGORITHM

According to Aoki Ta. et al. (1993) the signal output of the sensor at the *i*-th sampling during a scan of the etalon plate is written in the form:

$$V_i = C \int_{\nu_1}^{\nu_2} d\nu \phi_{FP}(\nu, t_i) \phi_B(\nu) [I_{refl}(\nu) + I_{path}(\nu)], \quad (1)$$

where *C* is the constant,  $\phi_{FP}$  is the transmission function of the tunable etalon,  $\phi_B$  is the transmission function of the narrow band pass filter,  $\nu_1$  and  $\nu_2$  are the lower and upper limits of the function  $\phi_B$ , respectively.  $I_{refl}$  is the radiance reflected at the surface and  $I_{path}$  is that scattered by the atmosphere.

In the near infrared region the path radiance  $I_{path}$  is one order of magnitude less than  $I_{refl}$  over the Lambertian surface whose albedo is about 0.05 when there is no absorption. However, to minimize the effect of the path radiance it is better to use the sun glint. The intensity of sun glitter radiance that is reflected into the view angle of about 0.5 degree is the order of  $10^{-3} \sim 10^{-5}$  of the incident radiation (Plass et al., 1977; Guinn, et al., 1979). This is  $10^4 \sim 10^2$  times larger than that over the Lambertian surface. Thus in case of sun glint  $I_{path}$  can be neglected compared to  $I_{refl}$ . Otherwise it can be taken into account based on, e.g., climatological values of aerosol distribution.

For an ideal etalon  $\phi_{FP}$  is given by the Airy function

$$\phi_{FP}(\nu, t) = \frac{(1 - r_{FP} - A_{FP})^2}{1 - 2r_{FP} \cos(2\pi\nu t) + r_{FP}^2}, \quad (2)$$

$$t = 2n_{FP}\delta \cos \gamma, \quad (3)$$

where  $A_{FP}$  is the absorptance of the etalon,  $r_{FP}$  is the reflectance of the surface of the etalon plate and  $n_{FP}$  is the refractive index of the medium between the etalon plates.  $\delta$  is the spacing between the two etalon plates and  $\gamma$  is the incident angle of the light. In this study  $\delta$  is changed by changing the voltage to be applied to the piezo elements.

The transmission function for the absorption due to molecules in a slant path is given by

$$\tau(\nu, \theta) = \exp\left[-\mu \int_0^\infty \sum_g k_{\nu,g}(z) \rho_g(z) dz\right], \quad (4)$$

$$\mu = \frac{1}{\cos \theta}, \quad (5)$$

where  $\theta$  is the zenith angle of the slant path,  $g$  stands for the species of the molecule,  $k$  is the absorption coefficient and  $\rho$  is the density.

We define a nondimensional quantity of the output signal for the  $i$ -th sampling by

$$F_i = \frac{V_i}{\bar{V}}. \quad (6)$$

For the normalization factor,  $\bar{V}$ , we take an average of measurements:

$$\bar{V} = \frac{1}{M} \sum_{i=1}^M V_i, \quad (7)$$

where  $M$  is the total number of the samples. It should be noted that  $F_i$  does not contain the constants  $C$  appeared in (1). This means that the absolute measurement of the intensity of radiation is not necessary in this method.

By expanding  $F_i$  around an initial guess we obtain

$$F_i(\delta_i) = F_i^\circ(\delta_i) + \sum_{j=1}^{N_0} \frac{\partial F_i}{\partial x_j} x_j, \quad (8)$$

$$y_i = F_{i,obs} - F_i^\circ = \sum_j K_{ij} x_j, \quad (9)$$

$$K_{ij} = \frac{\partial F_i}{\partial x_j}, \quad (10)$$

where  $F^\circ$  is the  $F$  theoretically calculated under the condition of the initial guess.  $x$  is the unknown parameter to be determined and the density of the  $j$ -th layer is given by

$$\rho_j = \rho_j^\circ(1 + \sigma_j x_j), \quad (11)$$

where  $\rho_j^0$  is the initial guess value for  $\rho_j$  and  $\sigma_j$  is the standard deviation of the error in initial guess, which was given artificially in the present work. This formula was used for making every  $x$  to be the same order. The unknown parameters are iteratively determined with the use of the maximum likelihood solution (Rodgers, 1976):

$$X_{(n+1)} = [S_x^{-1} + K_{(n)}^t S_\epsilon^{-1} K_{(n)}]^{-1} K_{(n)}^t \times S_\epsilon^{-1} [Y - Y_{(n)} + K_{(n)} X_{(n)}], \quad (12)$$

where  $X_{(n)}$  is the vector of  $x$  at the  $n$ -th step of the iteration,  $S_x$  is the covariance matrix of  $X$ ,  $K_{(n)}$  is the  $K$  appeared in (12) at the  $n$ -th step and  $S_\epsilon$  is the covariance matrix of the measurement error.

### III. GROUND BASED MEASUREMENTS

To examine the performance of the algorithm a ground based instrument has been developed for water vapor soundings. The block diagram of this instrument is shown in Fig.1. Since in this case we observe the direct solar radiation,  $I_{refl}$  in (1) becomes (Aoki et al., 1994),

$$I_{direct}(\nu) = I^\odot \phi^\odot(\nu) \Omega \tau, \quad (13)$$

where  $I^\odot \phi^\odot(\nu)$  is the extraterrestrial solar radiation, which may have a strong wavenumber dependence in the range between  $\nu_1$  and  $\nu_2$  due to absorption by the solar atmosphere. We assume that the absorption due to the solar atmosphere is well known so that we can give the extraterrestrial solar radiation with a constant  $I^\odot$  and a known function  $\phi^\odot(\nu)$ .  $\Omega$  is the solid angle of the field of view of the sensor. In the present study the view angle is 0.19 degree.

The transmittance spectra of the tunable etalon for some of the etalon plate spacing are shown in the top panel of Fig.2. An etalon and an interference filter together constitute a very narrow band pass filter as shown in the panel marked as "FILTER" in Fig.2. This band pass filter only covers a small wavenumber region which essentially contains only one absorption line of water vapor.

An example of the output signal of measurements is shown in Fig.3 for the case of the line at  $6541\text{cm}^{-1}$ , where the abscissa is the electric voltage applied to the piezo elements and the ordinate is the normalized output  $F_i$ . The solid line is the measurement and dashed one is the calculated. A deep dip of the curve corresponds to the water vapor absorption line at  $6541\text{cm}^{-1}$ . Two dips appear in the figure. This is because the continuous application of electric voltage from 0 to 1000 volt makes movement of the line of tunable etalon for more than one free spectral range.

The density profiles have been obtained by iteratively fitting the calculated curve of the normalized output to the measured one. Actual fitting has been made for the curves only within a narrow range of the voltage around one of two dips in Fig.3. The ground truth of the vertical profile of water vapor has been obtained within two hours from the radiosonde observation at the site far by about 100 meter. An example of retrieved profiles is shown in Fig.4. Here the thin solid line is the retrieval profile, the thick solid line is the profile from radiosonde observation, the dashed line is the initial profile and the thin solid line on the lefthand side of the figure is the difference between the retrieved and sonde observed profiles. It can be seen that the profile in the upper layers does not move greatly from the initial value. This is because the region around the absorption line center, where the information of the upper atmospheric layers is much involved, is completely absorbed and so it does not bring the information of the upper layers. To improve this we have to choose a line of weak line intensity.

Fig.5 is another example of measurement made in the Taklimakan Desert in China, where the water vapor amount is small (Aoki Te. et al., 1993). As seen in the figure, in this case the absorption at line center is not large and the profile of the upper troposphere

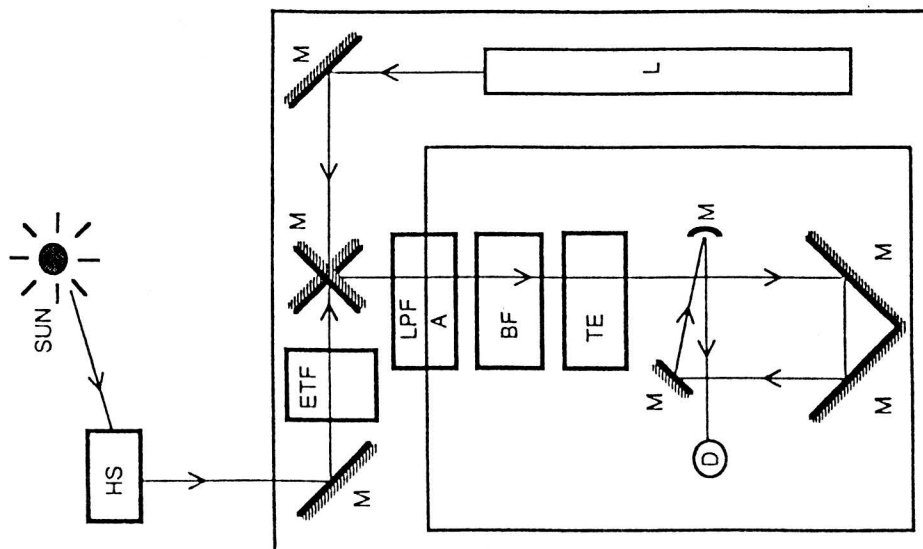


Fig.1 Block diagram of ground-based TERSE, where HS is the heliostat, ETF is the etalon, BF is the interference filter, TE is the tunable etalon and L is the HeNe laser.

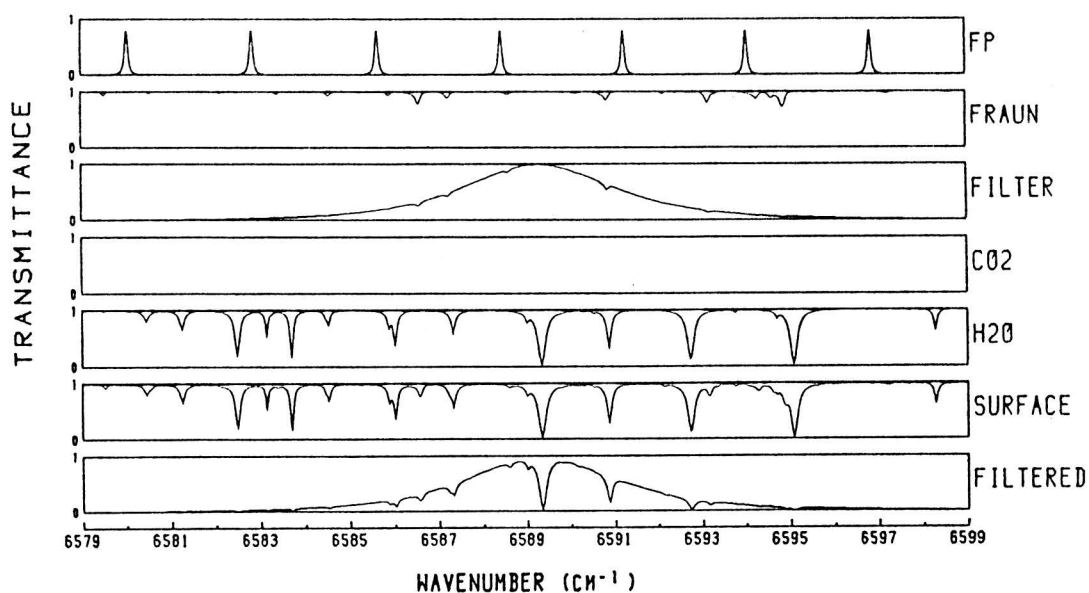


Fig.2 Spectra of the wavenumber region for the H<sub>2</sub>O sounding. The lowest two panels are the transmittance of the column atmosphere (the bottom panel is the filtered), the next two are those of the H<sub>2</sub>O and CO<sub>2</sub>, respectively. The panel signed as "FILTER" is the transmittance of the band pass filter. The next panel is the relative intensity of the extraterrestrial solar radiation and the top panel is that of the tunable etalon for some value of etalon plate separation.

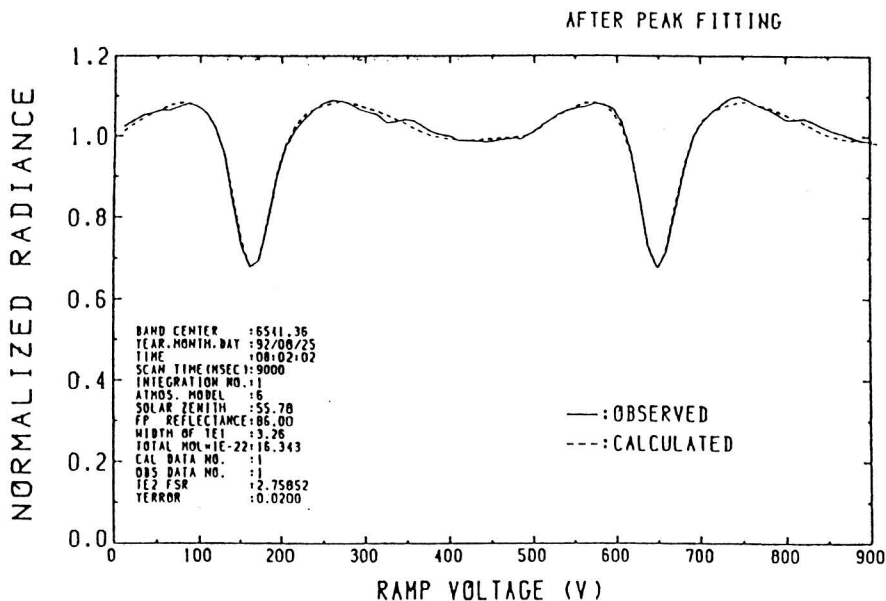


Fig.3 An example of the normalized output of measurement (solid line) with TERSE and calculated one (dashed line). The abscissa is the electric voltage given to the piezo element of the tunable etalon.

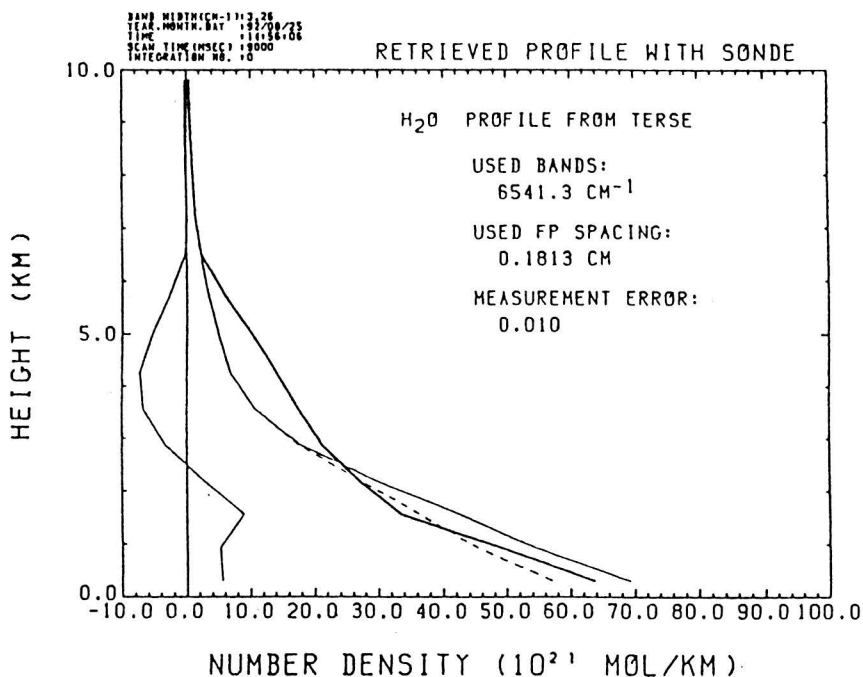


Fig.4 Comparison between retrieved vertical profile of water vapor (thin solid line) and sonde observation (thick solid line). The dashed line is the initial profile and the curve on the left hand side is the difference between retrieved and sonde observed profiles.

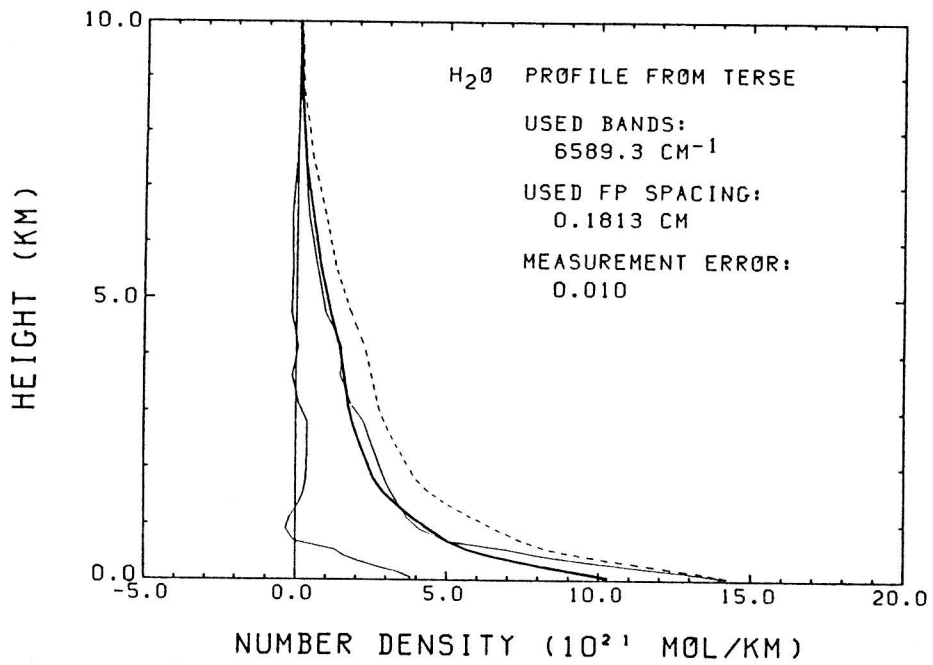


Fig.5 As in Fig.4 except for observation at Taklimakan Desert in China.

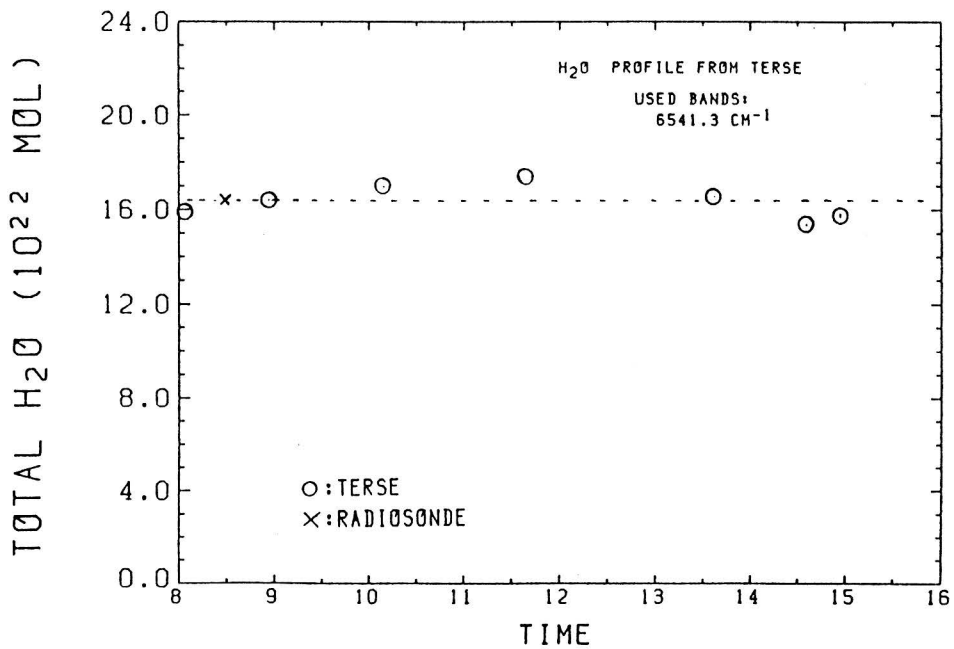


Fig.6 Diurnal variation of the total column amount of water vapor measured by TERSE.

is well retrieved. Fig.6 shows the diurnal variation of the total column amount of water vapor observed by TERSE. The sonde observation is shown by the mark of cross. It can be seen that inspite of the complete absorption of the part of the line center the total column amounts of water vapor are retrieved in good accuracy. The error is the order of a few percent.

#### REFERENCES

- Aoki Ta., A remote sounder for the vertical profiles of the atmospheric gases: simulation, *Proc. of Spring Meeting of Japan Meteorological Society, May 22-24, Tokyo, 62-62, 1989.* (in Japanese)
- Aoki Ta., Fukabori M., Aoki Te., Trace gas remote sounding from near IR sun glint observation with tunable etalons, *NATO Advanced Research Workshop "High Spectral Resolution Infrared Remote Sensing for Earth's Weather and Climate Studies"*, Springer-Verlag, Berlin, 309-322, 1993.
- Aoki Ta., Fukabori M., Aoki Te., Remote measurements of atmospheric constituents in the lower layers, *Proceedings of the International Symposium on "Global Cycles of Atmospheric Greenhouse Gases"*, Tohoku Univ., Sendai, Japan, 165-170, 1994.
- Aoki Te., Aoki Ta., Fukabori M., Remote sounding of the atmospheric water vapor at Hotan in Taklimakan Desert, *Proceedings of the Japan-China International Symposium on the "Study of the Mechanism of Desertification"*, Science and Technology Agency, Japan, 180-184, 1993.
- Guinn J. A., Jr., Plass G. N., Kattawar G. W., Sun glint glitter on a wind-ruffled sea: further studies, *Applied Optics*, 18, 842-849, 1979.
- Plass G. N., Kattawar G. W., Guinn J. A., Jr., Isophotes of sun glint glitter on a wind-ruffled sea, *Applied Optics*, 16, 643-653, 1977.
- Reichle H. G., Jr., Beck S. M., Haynes R. E., Hesketh W. D., Holland J. A., Hypes W. D., Orr III H. D., Sherrill R. T., Wallio H. A., Casas J. C., Saylor M. S., Gormsen B. B., Carbon monoxide measurements in the troposphere, *Science*, 218, 1024-1026, 1982.
- Rodgers C. D., Retrieval of atmospheric temperature and composition from remote measurements of thermal radiation, *Review of Geophysics and Space Physics*, 14, 609-624, 1976.
- Timchak A., Satellite-derived moisture profiles, *NOAA Tech. Rep. NESDIS*, 24, 1986.